The Effect of Shot-Peening on Stress Corrosion Cracking Behavior of Stainless Steel

Wang Renzhi, Li Xiangbin
and Yin Yuanfa

Institute of Aeronautical Materials
Beijing, China

ABSTRACT

The effects of the shot-peening on the stress corrosion cracking (SCC) of martensitic and austenitic stainless steels were investigated. It was conclude that higher dislocation density and the compressive residual stresses in the surface layer are two important factors which can improve the resistance to SCC for stainless steels, and the cleavage-like fracture of austenitic stanless steel in the case of SCC exhibits, in fact, a cleavage-like fracture of plastic induced martensite.

KEYWORDS

Shot-peening; Stress corrosion cracking; phase transformation; residual stress; fractography.

INTRODUCTION

The SCC is one of important failure mode of mechanical parts and components. It has been shown that tensile stress and aggressive enviroment to which the material is susceptible are two necessary conditions for producing SCC (Scully, 1975). It is obvious that the residual stresses (Pavlichko, 1978; Nakagawa, 1979) and the microstructural changes (Speidel, 1971) in the surface layer of materials exhibit a pronounced influence on the properties of SCC.

The surface strain strengthening by means of shot peening is often used to introduce compressive stresses into the surface layer and to change the surface microstructure of the materials, from which the resistance to SCC could be improved (ASM, 1975; Liu Sou, 1977). In the present paper the relationship between the property of SCC and the surface strengthening are investigated. The effects of both residual stresses and the surface microstructure changes on the SCC behavior of stainless steels are also discussed in detail.

MATERIALS AND EXPERIMENTAL PROCEDURES

The chemical compositions and the mechanical properties of both 1Cr18Ni9Ti austenitic (γ) and Cr17Ni2A martensitic (α') stainless steels used are listed in Table 1. The stress corrosion specimens were cut along rolling direction of the sheet, the size of which are 100x10x15mm. The surface pittings were conducted by means of electrochemical etching exposed in 0.1% NaCl solution, and the current density is 67 mA/cm^2 (10 min) at room temperature. The pitting depth is about 0.1-0.15 mm.

Table 1. Chemical composition and mechanical properties of two stainless steels

Material	Chemical composition (% by weight)								
	C	Mn	Si	S	P	Cr	Ni	Ti	Fe
1Cr18Ni9Ti	0.06	0.54	0.73	0.06	0.029	18.1	9.10	0.50	bal
Cr17Ni12A	0.145	0.38	0.50	0.11	0.33	17.0	2.21	-	bal

Material	Mechanical properties		
	Tensile strength MNm^{-2}	Yeld stress MNm^{-2}	Elongation %
1Cr18Ni9Ti	588	245	~50
Cr17Ni12A	1176	915	7-8

The stress corosion tests are performed using three point bending. The maximum bending stress of specimen is culculated by following formura:

$$\sigma_{max} = \frac{6Eh\rho}{L^2}$$

where ρ is the deflection (ρ=1.71-1.84 mm for γ steel, ρ=3.55-3.75 mm for α', these values correspond to 0.8 yield stress, σ_s, of both steels); h is the specimen thickness; L is the span; E is modules of elastisity.

During the stress corrosion tests, the γ specimens are exposed in 5N H_2SO_4+0.5N NaCl solution, and the α' specimens are discontinuously exposed in 3% NaCl solution with the rotating speed of 2 cycles per minute. All specimen surface are peened and the peened intensity is 0.19A (mm), using glass beats.

Both stress measurements and quantitative phase analysis are conducted with 2903 type X-ray diffractomether, using Cr-Kα and Cr-Kβ radiation. The observations of microstructure and fractographs are conducted on transimssion electron microscope (JEM-200A) and scanning electron microscope (JSM-35) respectively.

EXPERIMENTAL RESULTS

(1) Surface residual stresses

The amount and distribution of residual stresses, σ_r, existed in the surface layer of specimens after machining are quite different. Therefore the final surface stress at the center of specimen is, in fact, an algebraic sum of residual and applied stresses. The data summarized in Table 2 illustrate the changes in the surface stresses before and after loading for both stainless steels.

After shot peening, the phase transformation from γ to α' is experinced in the surface layer of γ steel, having a much higher surface compressive residual stresses. All date of σr for both steels before and after shot peening are shown in Fig.1 and Fig.2.

Table 2 Surface stresses before and after loading

Material	Surface state	Loading condition	Surface stress MNm^{-2}
1Cr18N19T1	before shot-peening	without loading	+294
		loading (ρ=1.78)	+490
		unloading	+235
	after shot-peening	without loading	-892
		loading (ρ=1.78)	-485
		unloading	-751
Cr17N12A	before shot-peening	without loading	0
		loading (ρ=3.75)	+608
		unloading	- 51
	after shot-peening	without loading	-706
		loading (ρ=3.75)	- 69
		unloading	-774

(2) Lifetime of stress corrosion rupture

Fig.1 shows the effect of shot peening on the lifetime of stress corrosion rupture (SCR), tr, for both smooth and pitting specimens of γ steel. For investigating the effect of individual microstructure, the peened specimens subject again to tensile plastic deformation (strain amount ε=1%) so that the residual stresses could be relaxed. The experimental results of the lifetime of SCR in the different surface states for α' steel are shown in Fig.2.

(3) Microstructure in the surface layer

It is well known that $\gamma \rightarrow \alpha'$ phase transformation can be induced by plastic deformation for metastable γ steels. The amount of transforming α' is dependent on the degree of plastic deformation, which is decreased gradually with the surface depth, as shown in Fig.3. It is seen from Fig.3 that the following tensile plastic deformation after peening (ε=0.3, 0.7 and 6.4%) do not affect the amount of α' . The micro-Vickers hardness of the transforming α' phase and γ phase are 460 and 275 repectively. Fig.4 shows the plastic induced α' lath in the surface strain layer, virgin austenite in the center as well as their electron diffraction patterns.

According to X-ray diffraction lines of α' in the different depth from the fracture surface for γ steel, it is found that the α' phase disappeares rapidly with the depth to about 1 μm. Thus, the depth of existence of transformed α' phase is about 1 μm. According to X-ray phase analysis, the amount of α' phase estimated in this depth would be more than 90%. This result is consistant with that obtained from the electron diffraction method (Liu, 1980). The variations of half width, β , of (211) lines and σr with the depth for α' steel are illustrated in Fig.5.

(4) Electrochemical property
The measurements of open potential, Vo, are summarized in Table 3.

(5) Morphology of fracture surface
The observations on the side smooth surface near the fracture surface of unpeened specimens for both steels indicate that a large number of small cracks exist on the surface, as shown in Fig.6. After shot peening, however, none of such small cracks was found at the same place. Fig.7 shows the fractographs of both smooth and peened specimens near the corrosion crack initiation zone for γ steel.

Table 3. Effect of microstructure and stresses on the value Vo for both stainless steels

Material	Test solution	Microstructure in the surface layer	Loading condition	Sum of residual and applied stresses MNm^{-2}	Vo mV
1Cr18Ni9Ti	5N H_2SO_4+ 0.5N NaCl	γ- phase	without loading	-83.3	-335
			loading	+167	-368
		plastic induced α'-phase	without loading	-647	-435
			loading	-706	-435
		α'-phase+tensile deformation	without loading	+25	-445
			loading	+167	-470
Cr17Ni2A	3% NaCl	undeformed α'-phase	without loading	0	+ 80
			loading	+675	+ 50
		plastic deformed α'-phase	without loading	-882	+160
			loading	-441	+140

DISCUSSION

From the experimental results it is evident that the changes in the SCC behavior of both steels are obviously connected with the microstructures and residual stress field in the surface layer.

(1) Martensitic stainless steel (Cr17Ni2A)
The saddle-like mode of $\beta-\delta$ curve, as in Fig.5, indicates that the microstructure in the surface layer subjects to cyclic softening and rehardening due to shot peening. As showing in the reference (Wang Renzhi, 1981), in the cyclic rehardening layer the subgrains are refined and dislocation density are increased due to plastic deformation, resulting in the difficulty of dislocation motion during following SCC.

It is shown from Fig.2 and Fig.5 that compressive residual stress field appears in the surface layer, the amount of which is about 800 MNm^{-2} in the surface. Both microstructure and residual stresses have strong influence on the electrochemical behavior. It is shown from Table 3 that the ratio $Vo/\Delta\sigma$ is 0.044~0.045 mV/MNm^{-2} for both smooth and peened specimens, from which the values Vo of both specimens under different surface stress conditions could be evaluated, as summarized in Table 4. The data lead to obtain following conclusions: (a) under zero surface stress, the value Vo of deformed α' phase is higher than that of virgin α' phase; (b) compressive stresses increase and tensile

stresses decrease the value Vo. In any case the materials having a higher Vo always appear to be a higher resistance to the electrochemical solusion (anodic solution).

The microstructure having a unbalanced dislocation distribution between subgrain boundaries and grains appears to be a higher electrochemical solution rate along the subgrain boundary. It can be seen from Fig.6, b that a large number of small cracks appear to be generated at subgrain boundary. The peened surface, however, could greatly increase dislocation density in the α' subgrain, producing a balanced dislocation between subgrains and its boundaries. The balanced dislocation distribution lead to minimize the difference of Vo values between them, resulting in a balanced electrochemical solution during stress corrosion test. In this case, no small crack in the vicinity of main crack was observed. Besides, the compressive residual stresses are another important factor which leads to increase the positive open potential Vo (Table 4), resulting in the improvement of resistance to SCC of martensite (Fig.2).

Table 4. The values Vo of deformed and undeformed phase for Cr17Ni12A steel

Microstructure in the surface layer	Loading condition	Surface stress MNm^{-2}	Open potential Vo mV
underformed phase	without loading	0	+ 80
	test loading	+735	+ 48
plastic deformed phase	without loading	0	+120
	without loading	-882	+160
	test loading	-147	+120

(2) Austenitic stainless steel (1Cr18Ni9Ti)
The previous investigations have been shown that tensile monotonic deformation at room temperature (Wang, 1982) or at -196°C (Birley, 1971) all can promte $\gamma \rightarrow \alpha'$ phase transformation of metastable γ steel. The cyclic plastic deformation can also induce such phase transformation, as shown in Fig.3. Fig.4 has been shown that the dislocation density in the martensite is much higher than that in the virgin austenite. The value Vo of α' phase is allways higher than Vo of γ phase regardless of the existence of compressive or tensile stresses in the surface (Table 3). This fact implise that α' phase exhibits a much higher electrochemical solution rate. However the unbalanced dislocation distribution in the virgin austenite could lead to concentrated stress corrosion, as showed in Fig.6,a. The transformed α' phase having a much higher dislocation density could effectively prevent the emergence of the small cracks near the main crack.

It is known that the plastic induced α' exhibits a higher tensile and yield strength. According to the micro-Vickers hardness number of α' (Hv=460), the tensile strength can be evaluated and the value is about 1500 MNm^{-2}. It is reasonable to consider that the yield strength is about 1000 MNm^{-2}. Under the same loading condition (i.e. ρ=1.8 mm), the applied maximum tensile stress σ_{max}=200 MNm^{-2} for vergin γ phase specimen and σ_{max}=400 MNm^{-2} for transtormed α' phase specimen respectively. It is obvious that the applied testing stress for α' phase

specimen is much lower than the yeild strength itself. This fact appers to be another factor which could extend the period of SCR.

The observations of fractographs show that the mud crack pattern near the surface for peened specimen and the depth of which is just equal to the depth which contains the amount of α' phase more than 30%. This mud crack pattern is, in fact, a corrosion products which are gradually formed during slow crack growth in the transformed α' phase. The tunnel pattern near the surface, as mentioned by Scully (1977), have been observed for unpeened specimen (Fig.7,a), but it no longer appears in the crack propagation zone. The fractographs in the crack propagation zone for both specimens have the same patterns which could be divided as follows: vane pattern, cleavage rivers and cleavage steps. The results of X-ray analysis of fracture surface lead to be the folowing conclusions: (a) γ phase subjects to plastic deformation due to crack propagation and the depth of which is about 2 μm; (b) the plastic induced α' appears in the surface fracture layer and the amount of which is more than 90%, distributing in about 1 μm depth. Consequently, it might be concluded that the cleavage-like fracture of the metastable austenitic stainless steel in the case of SCC exhibits, in fact, a cleavage-like fracture of plastic induced martensite. Thus the fracture process of stress corosion is a process of martensitic fracture but austenitic (Wang, 1982).

CONCLUSIONS

The results obtained may be summarized as follows:

1. Shot peening can be used to improve the resistance to SCC of both smooth and pitting specimens for austenitic and martensitic stainless steels.
2. High dislocation density and compressive residual stresses in the surface layer of the plastic induced α' are two important factors which can improve the resistance to SCC for austenitic stainless steel.
3. The cleavage-like fracture of austenitic stainless steel in the case of SCC exhibits, as a matter of fact, a cleavge-like fracture of plastic induced martensite.

REFERENCES

ASM Handbook committee (1975). Metal Handbook, Vol.10.

Birley, S.S. and D. Tromans (1971). Corrosion, 27, 62.

Liu Suo (1977). Fatigue of Metal Materials and shot-peening (in Chinese).

Liu, R., N. Narita, C. Altstetter, H. Birnbaum and E.N. Pugh (1980). Metall. Trans., 11A, 1563.

Nakagawa, Y.,K. Usami, A. Minato, T. Tamanura, R. Sasaki and A.Naruse (1979). Proceedings of Third International Conference on Mechanical Behavior Materials, 603.

Pavlichko, W.R., J.A. Begley, F.H. Beck and R.W. Staehle (1978). Microstructural Science, Vol.6, 229.

Scully, J.C. (1975). The Fundamentals of Corrosion, International Series on Materials Science and Technology, Vol. 17.

Scully, J.C. (1971). The Theory of Stress Corrosion Cracking in Alloys, NATO, 127.

Speidel, M.O. (1971). The Theory of Stress Corrosion Cracking in Alloys, NATO, 289.

Wang Renzhi, Li Xiangbin, Tan Yonggui and Yan Minggao (1981). Proceedings of First International Conference on Shot Peening, 185.
Wang Renzhi, Li Xiangbin, Yin Yuanfa and Yan Minggao (1982). J.of Aeronautical Materials, 2, 1 (in Chinese).

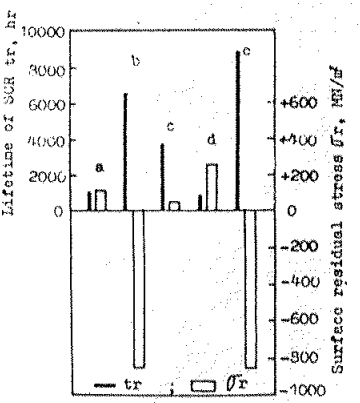

Fig.1 Stresscorrosion rupture and surface residual stresses for γ steel: a-smooth; b-smooth+peened; c-smooth+peened plastic deformation (ε=1%); d-pitting; e-pitting +peened.

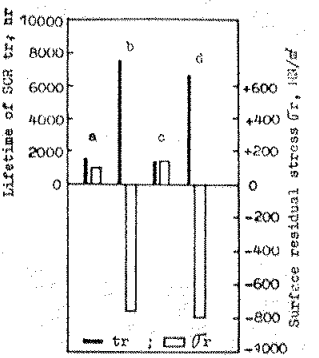

Fig.2 Stress corrosion rupture, residual stresses for α′ steel: a-smooth; b-smooth+peened; c-pitting; d-pitting+peened

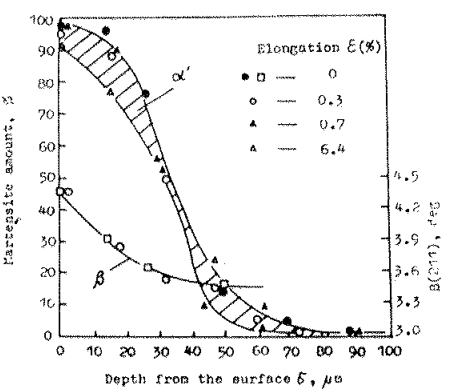

Fig.3 Distributions of the amount of transformed α′ phase and half width of (211) diffraction lines, β , with the depth, δ , for 1Cr18Ni9Ti

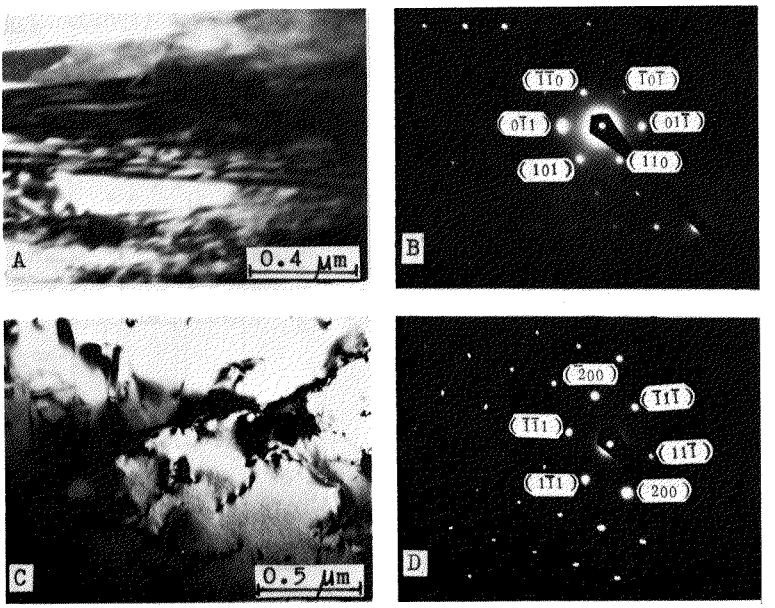

Fig.4 Transmission electron photographs for γ stell: a,b-transformed α' lath and its electron diffraction patern, Z=[011]; c,d-virgin γ phase and its electron diffraction pattern, Z=[1̄11]

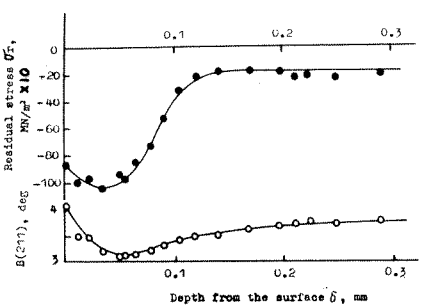

Fig.5 Variations of β of (211) lines and σr with depth for Cr17Ni2A steel

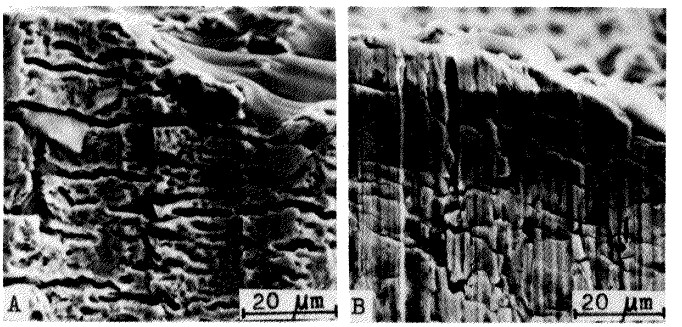

Fig.6 Scan electron photographs of small cracks at the side smooth surface for both unpeened steels: (a) 1Cr18Ni9Ti; (b) Cr17Ni2A

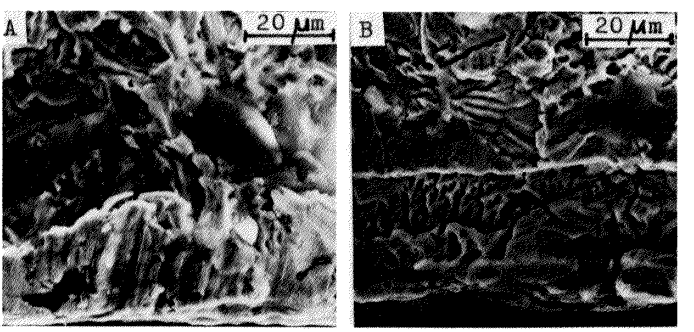

Fig.7 Scan electron fractographs near the crack initiation zone for 1Cr18Ni9Ti steel: (a) smooth; (b) smooth and peened